

AIR MASS EFFECTS ON THE CASSINI HIGH GAIN ANTENNA

Kenneth S. Smith* and Chia-Yen Peng†

*SDRC Operations, Inc.

11995 El Camino Real, Suite 200
San Diego, CA 92130

†Jet Propulsion Laboratory

California Institute of Technology
4800 Oak Grove Drive
Pasadena, CA 91109

ABSTRACT, *The high gain antenna for the Cassini spacecraft is a lightweight, large surface area structural element, and therefore its dynamic characteristics are noticeably altered by air mass effects. The virtual fluid mass approach as implemented in MSC/NASTRAN successfully accounts for lower natural frequencies observed in vibration testing. However, direct addition of air mass to the structural mass matrix during coupled loads analysis with the Titan IV/Centaur launch vehicle would give rise to unreasonably high static loading on the antenna. A correction to the air mass matrix was necessary to account properly for the fact that the bulk of air in the payload fairing is accelerated by the launch vehicle, not by the spacecraft. This correction was applied in a manner that allowed a traditional Craig-Bampton model of the spacecraft to be developed. Other than the air mass correction, no changes to the usual coupled loads analysis methodology were required*

NOMENCLATURE

- HGA High Gain Antenna
- DOF Degree(s) of freedom
- V Kinetic energy in dynamic system
- $\{x_g\}$ Displacement of model degrees of freedom
- $\{x_{,1}\}$ Displacement of spacecraft/upper stage interface degrees of freedom
- $\{x_{,j}\}$ Displacement of non-interface degrees of freedom
- $\{x_k\}$ Displacement of bulk air at model DOF
- $\{x_b\}$ 6-DOF rigid body displacement of air
- $[R_{gb}^a]$ Rigid body displacement column vectors
- $[T_{br}]$ Transformation from interface to 6-DOF rigid body
- $[M_{gs}^a]$ Air mass matrix from virtual fluid mass approach
- $[\tilde{M}_{gs}^a]$ Air mass matrix corrected for loads analysis
- $X(M)$ Fourier transform of transient displacement

1. INTRODUCTION

The Cassini spacecraft (Figure 1) will be launched on October 6, 1997, on a Titan IV/Centaur launch vehicle, and will reach Saturn in the year 2004. Cassini is by far the largest interplanetary spacecraft ever developed, with a total launch mass of 5600 kg. Propellants account for more than 3100 kg of this total.

The High Gain Antenna (HGA) at the top of the spacecraft will provide the primary communication link to the spacecraft over the 1.4 billion km distance between Earth and Saturn. The HGA, which was developed for the Cassini mission by the Italian Space Agency, is a fixed dish with a diameter of 4 m. The antenna structure utilizes carbon fiber rein-

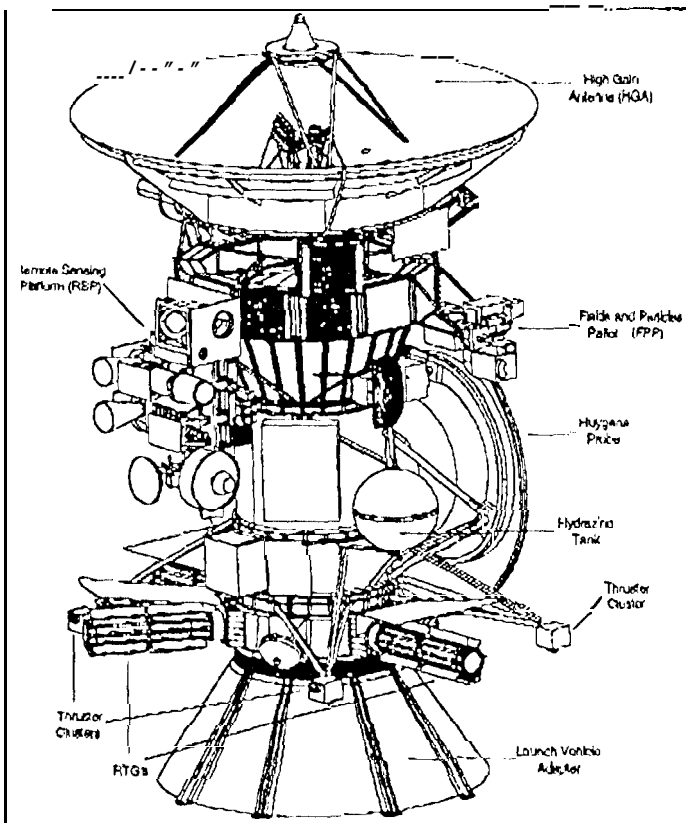


Figure 1. Cassini spacecraft launch configuration.

forced plate on an aluminum honeycomb core, resulting in a very small mass for such a large antenna. The total mass of the antenna and related hardware is approximately 105 kg.

This combination of low mass and large surface area makes the Cassini HGA susceptible to air loading effects during ground testing and during launch. The first indication that air loading was important came during sine vibration tests on the engineering model, when the fundamental natural frequency of the antenna was measured approximately 10% lower than predicted.

For a structure such as the Cassini HGA, the primary effect of the surrounding air is to add mass to the surface of the antenna. Some amount of air surrounding the antenna must be accelerated along with the structure, and this results in the added mass effect. As a result, the natural frequencies of the antenna in air tend to be lower than in vacuum. The air mass effect is strongest on global modes of the structure, since a greater quantity of air must be accelerated. The higher order modes are only slightly affected. Rough assessment of the air mass confirmed that it could account for the observed frequency drop.

It is important to quantify air mass effects properly, so that the dynamic loads on the antenna can be predicted. Ultimately, antenna loads are estimated by performing a coupled response analysis of the combined launch vehicle, upper stage, and spacecraft under static and transient loading. An understanding of the effect of air is necessary even for dynamic events late in the launch sequence (when no air is present), since the mode must be appropriately changed from the ground test configuration.

This paper describes the method ultimately used to quantify these effects on the Cassini HGA. Since the calculation of air mass has been documented in previous work, that aspect of the work is not detailed herein. Instead, this paper concentrates on the method of application of the added mass to the dynamic model of the spacecraft. It was discovered that a correction to the added mass was necessary to avoid inappropriate static loading on the antenna. The correction was applied in such a way that the dynamic model could be treated normally for coupled analysis by the launch vehicle contractor.

2. VIRTUAL FLUID MASS APPROACH

The virtual fluid mass method in MSC/NASTRAN [1] was developed to account for structures immersed in fluids, such as ships. The formulation assumes the fluid is incompressible, and involves distributing point sources appropriate to the finite element mesh of the wetted portion of the surface. The virtual mass generation module produces a mass matrix corresponding to the wetted degrees of freedom. This air mass matrix is fully populated, and is added to the structural mass matrix prior to eigenvalue solution.

Tests performed in a vacuum chamber by Hughes Aircraft Company on the Intelsat VI C-Band transmit reflector [2] established that even with the assumption of incompressibility, the virtual fluid mass formulation in MSC/NASTRAN accurately accounted for the natural frequency shifts observed in the actual structure. Since the Intelsat reflector was structurally very similar to the Cassini HGA, the same approach was used with confidence for this application. The air medium was taken as infinite in extent, and both sides of the elements were wetted.

The air mass matrix generated by MSC/NASTRAN totaled approximately 33 kg of added mass in the vertical direction, and only 2 kg of added mass in the lateral direction (due to the orientation of the antenna surface). The air mass is distributed across the surface of the reflector, and is fully populated (i.e., there is mass coupling between all surface degrees of freedom). Table 1 shows the effect that the air mass matrix has on the first twelve natural frequencies of the antenna.

Table 1, HGA natural frequencies in vacuum and in air.

Mode	Frequency (Hz)		Percent Difference
	Vacuum	1 Atm	
1	39.42	36.19	-8.2
2	40.00	36.68	-8.3
3	49.08	47.55	-3.1
4	50.13	48.53	-3.2
5	54.71	51.53	-5.8
6	55.42	55.14	-0.5
7	56.99	56.74	-0.4
8	58.36	57.92	-0.7
9	62.55	62.54	0.0
10	64.28	64.07	-0.3
11	75.71	70.74	-6.6
12	76.03	71.01	-6.6

Because the Cassini finite element model has been developed in UAI/NASTRAN, some extra effort was necessary to achieve the same result. UAI/NASTRAN has no virtual fluid mass capability, so the air mass matrix computed in MSC/NASTRAN (using the HGA submodel only) was written to DMIG cards for inclusion in the UAI/NASTRAN data deck. These mass terms were then added directly to the structural mass during matrix generation. Because the air mass matrix is full, the resulting card deck was substantial. To minimize the size of the air mass matrix, the virtual mass calculation was performed with only the main reflector dish elements wetted. The frequencies resulting from the full application and partial application of air mass were found to be acceptably close.

The virtual mass computation was done with the air density set to its value at one atmosphere. Since the air mass matrix

is proportional to the density of the fluid, the same matrix could be used for any desired density, simply by multiplying by a scale factor. This was accomplished by a simple alter to the solution sequence where the full mass matrix is assembled as the sum of the structural mass and the air mass,

3. APPLICATION TO LAUNCH ENVIRONMENT

The direct addition of the air mass matrix to the structural mass matrix properly accounts for the changes to the natural frequencies and the mode shapes of the antenna when surrounded by air. However, it is not hard to see that this approach is not entirely accurate for modeling the launch environment.

Imagine the entire launch vehicle undergoing static acceleration of 1 g in the axial direction. The antenna support structure must carry the 105 kg weight of the antenna, but the air inside the fairing should not add any load in the antenna. Under steady acceleration, the air will reach equilibrium, and the pressure on both sides of the antenna surface will cancel. With the air mass added to the antenna surface DOF. however, the finite element model will add the 33 kg of air mass to the antenna structural mass, resulting in additional structural loads. This load is actually carried by the payload fairing, which is accelerating all of the enclosed air. Clearly, simple matrix addition does not adequately account for static loading effects,

The reason for the static loading error lies in the basic formulation of the equation of motion involving the air mass. Proper formulation results in a correction to the air mass matrix as explained in the following section,

4. AIR MASS MATRIX STATIC CORRECTION

Direct addition of the air mass matrix to the structural mass matrix is appropriate for forced response problems in which the air medium is not accelerating. In such a case, the kinetic energy of the air is

$$V = -\frac{1}{2} \{\dot{x}_g\}^T [M_{gg}^a] \{\dot{x}_g\},$$

where $\{\dot{x}_g\}$ is the velocity of the degrees of freedom of the model, and $[M_{gg}^a]$ is the air mass matrix computed from the virtual fluid mass formulation. When equation (1) is added to the kinetic energy from the structural mass matrix, the result is that the air mass matrix $[M_{gg}^a]$ gets directly added to the structural mass matrix.

This formulation is not valid in the launch environment, as discussed in the previous section. The correct formulation can be derived by noting that the forces of the air on the structure are proportional not to the absolute accelerations of

the grid points, but to their accelerations relative to the acceleration of the bulk of air. Thus the kinetic energy of the air would be

$$V = \frac{1}{2} \{\dot{x}_g - \dot{r}_g\}^T [M_{gg}^a] \{\dot{x}_g - \dot{r}_g\}, \tag{2}$$

where $\{\dot{r}_g\}$ is the velocity of the bulk of air at the grid points of the model. The bulk of air should move along with the payload fairing. The most correct way to do this would be to use the rigid body modes of the coupled dynamic system to derive the quasi-static motion of the air. However, such a formulation would require modification to the standard coupled loads processing, at a substantial cost and risk. Instead, we will assume the bulk of air moves together with the average rigid body motion of the Cassini/Centaur interface. This assumption, while not perfectly accurate, has the benefit of allowing the problem to be formulated entirely with spacecraft DOF, and therefore the correction can be done within the spacecraft model itself,

The bulk air rigid body motion $\{r_g\}$ can be written as

$$\{r_g\} = [R_{gb}] \{x_b\}. \tag{3}$$

where $\{x_b\}$ is an imagined 6-DOF grid point whose displacement describes the position of the bulk of air. The columns of $[R_{gb}]$ are the 6 rigid body displacement vectors at the grid points of the model resulting from motion at the reference point. The matrix $[R_{gb}]$ is easily derived from geometry of the model. Based on the assumption that the bulk of air moves with the Cassini/Centaur interface, we can further express $\{x_b\}$ in terms of the displacements of the Cassini/Centaur interface degrees of freedom, $\{x_r\}$:

$$\{x_b\} = [R_{rb}^T R_{rb}]^{-1} [R_{rb}]^T \{x_r\} \equiv [T_{br}] \{x_r\}. \tag{4}$$

(1) This least-squares solution is identical to the formulation of the RBE3 element in MSC/NASTRAN. Now if we merge the columns of $[T_{br}]$ with zeros for the remaining degrees of freedom, we can write

$$\{x_b\} = [T_{bg}] \{x_g\}, \tag{5}$$

where

$$[T_{bg}] = [T_{br} \quad 0_{bf}]. \tag{6}$$

(The subscript f represents all non-interface DOF.) Inserting equation (5) into equation (3) then gives

$$\{r_g\} = [R_{gb} T_{bg}] \{x_g\}. \tag{7}$$

Thus the bulk air motion at each surface degree of freedom is now expressed in terms of the displacements of the structural degrees of freedom. Returning to equation (2), the kinetic energy of the air can now be expressed as

$$\begin{aligned} V &= \frac{1}{2} \left\{ \dot{x}_g \right\} - [R_{gb} T_{bg}] \left\{ \dot{x}_g \right\} \left[M_{gg}^a \left\{ \dot{x}_g \right\} - [R_{gb} T_{bg}] \left\{ \dot{x}_g \right\} \right] \\ &= \frac{1}{2} \left\{ \dot{x}_g \right\}^T \left[I_{gg} - R_{gb} T_{bg} \right]^T \left[M_{gg}^a \right] \left[I_{gg} - R_{gb} T_{bg} \right] \left\{ \dot{x}_g \right\} \\ &= \frac{1}{2} \left\{ \dot{x}_g \right\}^T \left[\tilde{M}_{gg}^a \right] \left\{ \dot{x}_g \right\}, \end{aligned} \tag{8}$$

where

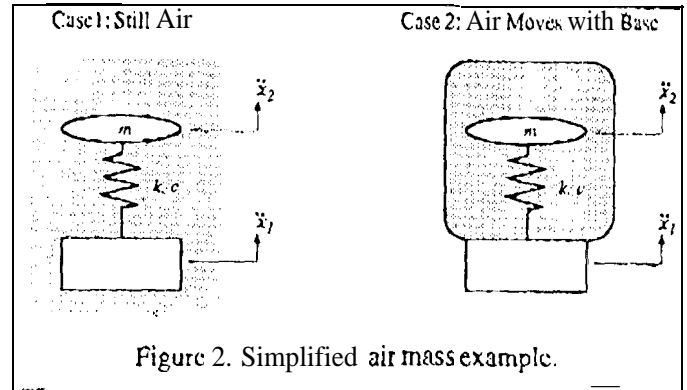
$$\left[\tilde{M}_{gg}^a \right] = \left[I_{gg} - R_{gb} T_{bg} \right]^T \left[M_{gg}^a \right] \left[I_{gg} - R_{gb} T_{bg} \right]. \tag{9}$$

The corrected air mass matrix $\left[\tilde{M}_{gg}^a \right]$ takes the place of the original air mass matrix in the equations of motion. This correction is applied to the air mass matrix prior to adding it to the structural mass matrix, and eliminates the static overloading error. After the corrected air mass matrix is incorporated, the model can be processed in the usual way to prepare for coupled loads analysis. For Cassini, a Craig-Bampton component mode of the spacecraft was prepared and delivered to the launch vehicle contractor for the final pre-launch coupled loads analysis. The mass matrix correction was incorporated in the Craig-Bampton DMAP program.

One feature of the air mass correction of equation (9) that is not immediately obvious is that the partition of the matrix associated with non-interface DOF (the *f*-set) remains unchanged. As a result, the cantilevered frequencies and mode shapes of the spacecraft are the same with or without the correction. The correction does change terms in the interface partition of the mass matrix, which affect the coupling of the spacecraft to the launch vehicle.

5. SIMPLIFIED EXAMPLE

A simplified example will help clarify how the above equations affect the dynamics of a structure. The example consists of a single degree of freedom mass on a spring, which is excited by base motion. The mass is imagined to be a flat disk which is immersed in air. Figure 2 illustrates the two cases to be considered. On the left side of the figure (case 1), the base motion and mass motion are assumed to take place in unmoving air. In this case, the air mass forces are proportional to the absolute acceleration of the mass. On the right side of the figure (case 2), the air is driven along with the base, and the air mass forces are proportional to the relative acceleration of the mass.



In both cases, let x_b be the displacement of the base, and x_2 be the displacement of the disk. Let m_a be the virtual mass of the air acting on the disk.

In case 1, the equation of motion is

$$\begin{bmatrix} 0 & 0 \\ 0 & m + m_a \end{bmatrix} \begin{Bmatrix} \ddot{x}_1 \\ \ddot{x}_2 \end{Bmatrix} + \begin{bmatrix} c & -c \\ -c & c \end{bmatrix} \begin{Bmatrix} \dot{x}_1 \\ \dot{x}_2 \end{Bmatrix} + \begin{bmatrix} k & -k \\ -k & k \end{bmatrix} \begin{Bmatrix} x_1 \\ x_2 \end{Bmatrix} = \begin{Bmatrix} f \\ 0 \end{Bmatrix}. \tag{10}$$

This can be readily solved in the frequency domain to obtain the reaction force $k(x_2 - x_1)$ in the spring, for a given base acceleration:

$$\begin{aligned} k(X_2(\omega) - X_1(\omega)) &= \\ &= \left(m + \frac{m_a \omega^2}{-\omega^2 + 2i\zeta\omega_0\omega + \omega_0^2} \right) X_1(\omega), \end{aligned} \tag{11}$$

where

$$\omega_0 = \sqrt{\frac{k}{m + m_a}}; \quad \zeta = \frac{c}{2\sqrt{k(m + m_a)}}. \tag{12}$$

Thus, as expected, the effect of the air mass term m_a under normal circumstances (case 1) is both to lower the natural frequency of the system and to increase the loading on the spring.

Now consider the second case, which is more representative of the launch condition. The equations in the previous section can be applied easily, and have the following results (letting x_1 be the base reference):

$$\left[R_{gb} \right] = \begin{bmatrix} 1 \\ 1 \end{bmatrix}. \tag{13}$$

$$\left[R_{rb} \right] = [1]. \tag{14}$$

$$\left[T_{br} \right] = \left[R_{rb}^T R_{rb} \right]^{-1} \left[R_{rb} \right]^T = [1]. \tag{15}$$

$$[T_{bg}] = [1 \ 0]. \tag{16}$$

$$[I_{gg} - R_{gb}T_{bg}] = \begin{bmatrix} 1 & 0 \\ 0 & 1 \end{bmatrix} - \begin{bmatrix} 1 & 0 \\ 1 & 0 \end{bmatrix} = \begin{bmatrix} 0 & 0 \\ -1 & 1 \end{bmatrix}. \tag{17}$$

$$[\tilde{M}_{kk}^a] = \begin{bmatrix} 0 & -1 \\ 0 & 1 \end{bmatrix} \begin{bmatrix} 0 & 0 \\ 0 & m_a \end{bmatrix} \begin{bmatrix} 0 & 0 \\ -1 & 1 \end{bmatrix} = \begin{bmatrix} m_a & -m_a \\ -m_a & m_a \end{bmatrix}. \tag{18}$$

Thus the equation of motion for case 2 is as follows;

$$\begin{bmatrix} m_a & -m_a \\ -m_a & m_a + m_a \end{bmatrix} \begin{Bmatrix} \ddot{x}_1 \\ \ddot{x}_2 \end{Bmatrix} + \begin{bmatrix} c & -c \\ -c & c \end{bmatrix} \begin{Bmatrix} \dot{x}_1 \\ \dot{x}_2 \end{Bmatrix} + \begin{bmatrix} k & -k \\ -k & k \end{bmatrix} \begin{Bmatrix} x_1 \\ x_2 \end{Bmatrix} = \begin{Bmatrix} f \\ 0 \end{Bmatrix}. \tag{19}$$

No[ice that the lower right partition of the matrices are identical to equation (10). The correction changes the coupling of the base to the mass, while leaving the fixed-base dynamics unchanged, Solving equation (19) in the frequency domain for the spring reaction force gives

$$k(X_2(\omega) - X_1(\omega)) = m \frac{-\omega_0^2}{-\omega^2 + 2i\zeta\omega_0\omega + \omega_0^2} X_1(\omega), \tag{20}$$

where ω_0 and ζ are identical to their values in equation (12) for case 1.

Comparing equations (11) and (2.0), it can be seen that in case 2 the air mass shifts the frequency of the system exactly as it does in case 1, but that the reaction force is multiplied only by the structural mass. This is true both for quasi-static accelerations ($\omega \rightarrow 0$) and at resonance, because in case 2 the base does the work of accelerating the bulk of the air.

Note that the distinction between the two cases applies only to base excitation. If the base is fixed and excitation is applied directly to the mass, then both equations of motion are the same and therefore give the same result.

A final observation can be made regarding the reaction force at the base. In equation (10) for case 1, the lower partition shows that the reaction force f at the base is equal to the spring force $k(x_2 - x_1)$ plus the damper force. In equation (19) for case 2, however, there is an additional term $m_a(\ddot{x}_1 - \ddot{x}_2)$ which adds to the interface force. This means that in this formulation, the additional mass m_a , while not transmitted through the structure, is still passed through the interface. For the Cassini HGA, this means that the air mass adds static load to the Centaur upper stage, but not the Cassini structure. This is a direct consequence of the assumption that the bulk of air moves with the interface. This load should really be carried by the fairing. Even so, the

impact of [his approximation on Centaur loads should be negligible, comparing the 33 kg air mass to the 5600 kg mass of the full spacecraft,

6. PREDICTED EFFECT ON HGA LOADS

Three different versions of the HGA model were created to demonstrate the effect of air mass and the air mass correction on loads. The first model was for [he antenna in a vacuum, with no air mass at all, The second version was with air mass at 1 atmosphere. with the correction applied as described in section 4, The third version was with the 1 atmosphere air mass matrix directly added to the structural mass matrix without correction.

For each case, the antenna support bipeds were fixed in a ground reference, and the system was driven by sinusoidal ground r-motion in the X, Y, and Z directions separately. The summed reaction forces in the support bipeds were recovered at each frequency in the excitation direction. This is the "apparent mass" of the antenna on its bipeds. The results for each of the three directions as a function of excitation frequency are shown in Figures 3 through 5,

The plots show the frequency shifts that occur between the vacuum and 1 atmosphere models. Even the fundamental lateral modes (X and Y directions) are shifted, because of the dish motion associated with the lateral modes,

Very little difference can be seen between the corrected and uncorrected results in the lateral direction, because the lateral air mass is so small. However, the effect of the correction is clearly visible in the vertical direction (Figure 5). The uncorrected model produced higher loads at low frequencies, corresponding to the 33 kg of air mass, This demonstrates that the mass correction successfully removes the quasi-static loading of the air mass,

At the 80 Hz resonance in Figure 5, the corrected model produces a load comparable to that of the vacuum model at its corresponding 88 Hz resonance, The uncorrected model shows a higher loading at resonance, although, the corrected and uncorrected models have the same natural frequency. This means that the added air mass does not inherently increase the loads in the antenna at resonance, the way a simple lumped mass addition would. These features are consistent with the simplified example.

Based on this study, the net effect of the air mass is expected to be limited to a shift of the frequencies of the antenna, with no tendency to increase the loading on the antenna structure. However, the frequency shift itself might cause increased loads, due to adverse coupling with the rest of the spacecraft.

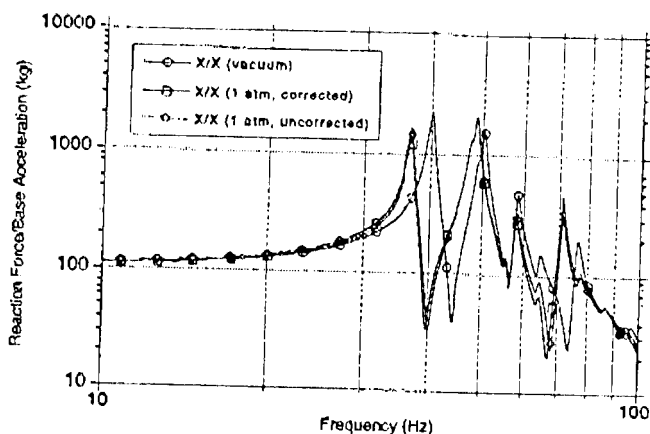


Figure 3. Apparent mass of HGA in X direction (lateral),

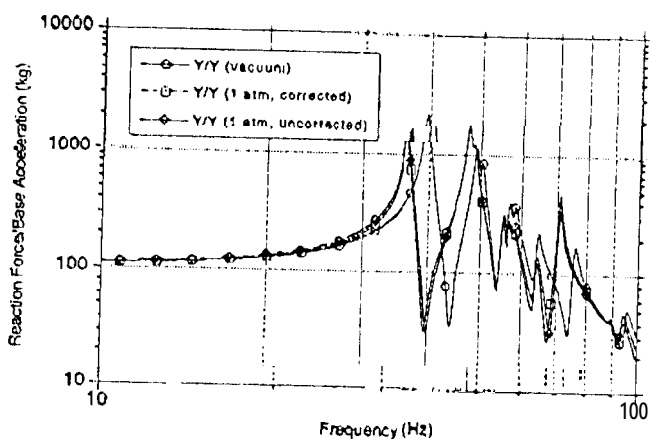


Figure 4. Apparent mass of HGA in Y direction (lateral).

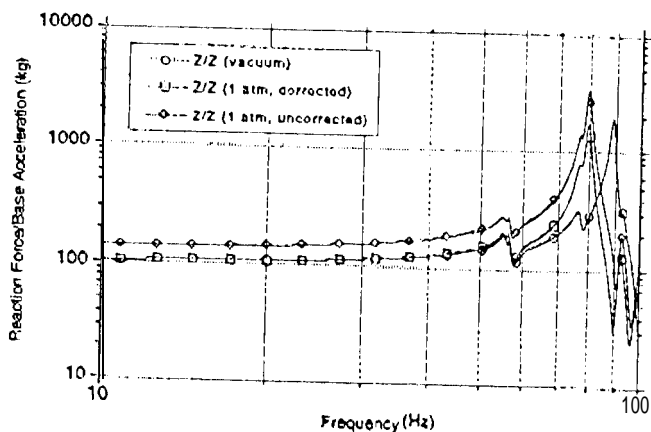


Figure 5. Apparent mass of HGA in Z direction (vertical).

7. STRATEGY FOR MULTIPLE LAUNCH EVENTS

The methodology described above allowed the proper inclusion of air mass effects in the Cassini spacecraft dynamic model. However, the situation is somewhat complicated by the fact that the air density inside the payload fairing is continually decreasing during the launch. During the time of critical aerodynamic loading (between 35 and 60 seconds after liftoff), the air density falls from 72% to 38% of its value at liftoff. Coupled loads analyses are performed for three different time points during this critical launch phase.

In principle, each of these analyses would require the preparation of a different spacecraft model, because [the air mass would be different at each time. These models would be in addition to the liftoff model (with 100% air density) and the later staging events (with no air mass),

The decision was made to use a single spacecraft model for all three aerodynamic loading events, with air density set to 50% of liftoff. This compromise meant that "only" three Craig-Bampton models needed to be generated. A study was performed to validate that the 50% model was sufficiently similar to the 38% and 72% models.

8. SUMMARY

Because of its light weight and large surface area, the Cassini HGA was susceptible to air mass effects, which dropped its natural frequencies by up to 10%. Direct addition of air mass to the structural mass did not properly account for the true physics of the launch environment, however. A method was developed to correct the air mass matrix to account for the fact that the payload fairing is accelerating the bulk of the enclosed air. With this correction, the effect of air mass on the antenna loads is limited to a frequency shift, with no inherent increase in static loads or apparent mass at resonance.

ACKNOWLEDGEMENT

The work described herein was conducted by the Jet Propulsion Laboratory, California Institute of Technology, under contract with National Aeronautics and Space Administration.

REFERENCES

- [1] "Functional Module MGEN (Fluid Mass Generation)," MSC/NASTRAN Programmer's Manual, Volume IV, section 4.184-1, January 31, 1981.
- [2] J. Fowler, et. al., "Effect of Air Mass on Modal Tests," proceeding of the 5th International Modal Analysis Conference, pp.1078-1083, London, England, April 6-9, 1987.